Stem Cell Reports
Report
ISSCR
OPEN ACCESS

Estrogen Receptor β Controls Muscle Growth and Regeneration in Young Female Mice

Daiki Seko,[1,2,6] Ryo Fujita,[2,3,6,7] Yuriko Kitajima,[2] Kodai Nakamura,[1] Yuuki Imai,[4] and Yusuke Ono[1,2,5,*]
[1]Department of Muscle Development and Regeneration, Institute of Molecular Embryology and Genetics, Kumamoto University, 2-2-1 Honjo, Kumamoto 860-0811, Japan
[2]Nagasaki University Graduate School of Biomedical Sciences, Nagasaki, Japan
[3]Department of Human Genetics, McGill University, Montreal, QC, Canada
[4]Division of Integrative Pathophysiology, Proteo-Science Center, Graduate School of Medicine, Ehime University, Ehime, Japan
[5]Center for Metabolic Regulation of Healthy Aging, Kumamoto University Faculty of Life Sciences, Nagasaki, Japan
[6]Co-first author
[7]Present address: Division of Regenerative Medicine, Transborder Medical Research Center, University of Tsukuba, Ibaraki, Japan
*Correspondence: ono-y@kumamoto-u.ac.jp
https://doi.org/10.1016/j.stemcr.2020.07.017

SUMMARY

Estrogens are female sex hormones that are important for comprehensively maintaining muscle function, and an insufficiency affects muscle strength and regeneration in females. However, it is still unclear whether estrogen signaling is mediated through receptors. To investigate the specific role of estrogen receptor β (ERβ) in skeletal muscle and satellite cells (muscle stem cells), we generated muscle-specific ERβ-knockout (mKO) and satellite cell-specific ERβ-knockout (scKO) mice, respectively. Young female mKO mice displayed a decrease in fast-type dominant muscle mass. Female, but not male, scKO mice exhibited impaired muscle regeneration following acute muscle injury, probably due to reduced proliferation and increased apoptosis of satellite cells. RNA-sequencing analysis revealed that loss of ERβ in satellite cells altered gene expression of extracellular matrix components, including laminin and collagen. The results indicate that the estrogen-ERβ pathway is a sex-specific regulatory mechanism that controls muscle growth and regeneration in female mice.

INTRODUCTION

Skeletal muscle is a highly plastic tissue that responds to various extrinsic stimuli, such as exercise, to adapt to muscle mass and strength. However, muscle mass and strength are decreased in pathological conditions, including aging, resulting in disability and poor quality of life. Skeletal muscle homeostasis depends on the activity of muscle-specific stem cells called satellite cells (Mauro, 1961), which are mitotically quiescent and express the paired homeodomain transcriptional factor PAX7 in normal physiological conditions (Brack and Rando, 2012; Relaix and Zammit, 2012). Upon muscle injury or diseases, satellite cells respond quickly to activate myogenic programming and proliferate, eventually fusing together to make new muscle fibers. Some of the progeny of the activated satellite cells undergo self-renewal by asymmetric division mechanisms to maintain the stem cell pool. With aging, the ability and the number of satellite cells to repair injured muscles is progressively impaired due to the alterations in both niche environment and cell-intrinsic mechanisms, which ultimately hinder skeletal muscle homeostasis (Kuang and Rudnicki, 2008; Tierney and Sacco, 2016). However, the molecular mechanisms of the aging-related disruption of the regenerative capacity of satellite cells are unclear.

Many lines of evidence have shown that hormones, including thyroid hormone, glucocorticoid, and sex hormones (androgens and estrogens), have an impact on skeletal muscle mass and strength (Seko et al., 2016; Shimizu-Motohashi et al., 2015; Sinha-Hikim et al., 2006; Sipila and Poutamo, 2003). Estrogens play important roles in muscle regeneration after injury as well as maintaining muscle mass and strength in females (Diel, 2014). Estrogens attenuate muscle injury by suppressing inflammation (Tiidus et al., 2001; Velders et al., 2012). The number of satellite cells is increased by estrogen administration during muscle regeneration *in vivo* (Enns and Tiidus, 2008). Estrogens stimulate myofibers to establish the quiescent satellite cell pool in muscle regeneration (Kim et al., 2016). Ovariectomy (OVX)-induced estrogen insufficiency results in a delay in the recovery of muscle mass after reloading following suspension-induced muscle atrophy (McClung et al., 2006; Sitnick et al., 2006). Recently, we reported that estrogens are crucial for muscle growth as well as satellite cell functions in young female mice (Kitajima and Ono, 2016). These findings suggest that estrogens have a variety of roles in alleviating disuse-induced muscle atrophy, promoting regrowth after reloading, and in muscle regeneration. Because 17β-estradiol (E2) levels in the blood sharply decline after menopause in women, it is plausible to postulate a direct impact of estrogens on skeletal muscle tissues and satellite cells.

Estrogen receptors (ERs) are expressed in a variety of organs, including skeletal muscle and myoblasts, in mice and in humans (Baltgalvis et al., 2010; Wiik et al., 2009). There are two types of estrogen receptors, ERα and ERβ.

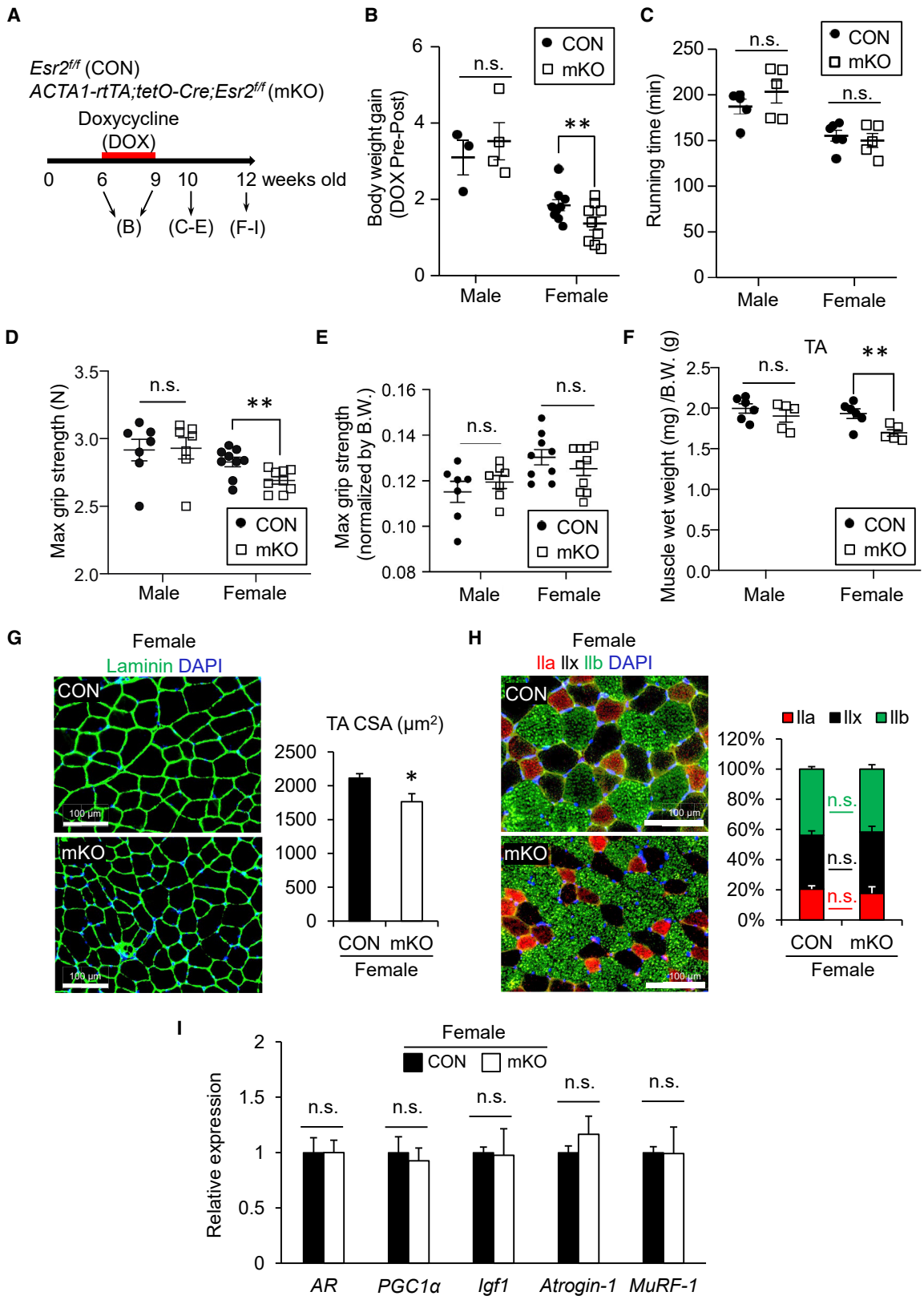

(legend on next page)

Both are nuclear transcriptional factors involved in various cellular functions, with common and different roles, and distinct effects (Hamilton et al., 2017). Recent studies demonstrated that ERα is involved in mitochondrial integrity (Ribas et al., 2016), lipid metabolism (Schweisgut et al., 2017), atrophy (Ogawa et al., 2015), and regeneration (Collins et al., 2019) in skeletal muscle. Although E2 preferably binds to ERα, we have found that consecutive intake of soymilk containing isoflavones, which preferentially bind to ERβ, ameliorated muscle atrophy and satellite cell dysfunction in ovariectomized female mice (Kitajima et al., 2017; Kitajima and Ono, 2016), suggesting that ERβ signaling is also a factor that regulates both skeletal muscles and satellite cells. However, the roles of ERβ in skeletal muscle and satellite cells are poorly understood. Here, we report the role of ERβ in skeletal muscle and satellite cells using muscle- and satellite cell-specific ERβ knockout (KO) mice.

RESULTS

Muscle-Specific ERβ Ablation Results in Reduced Muscle Mass and Strength in Young Female Mice

Since ERβ is expressed in skeletal muscles (Wiik et al., 2009), we first assessed whether ERβ is responsible for the maintenance of muscle function. To investigate the direct function of ERβ in muscles of young male and female mice, we generated doxycycline (DOX)-inducible and muscle-specific ERβ-KO mice by crossing *ACTA1-rtTA;tetO-Cre* mice (Rao and Monks, 2009) with *Esr2*-floxed (*Esr2*$^{f/f}$) mice (Antal et al., 2008). *ACTA1-rtTA;tetO-Cre;Esr2*$^{f/f}$ mice were treated with DOX (2 mg/mL) for 3 weeks to induce genetic inactivation of ERβ (mKO) (Figures 1A and S1A). *Esr2*$^{f/f}$ mice were used as a control (CON). The body weight was reduced to 30% of female mKO mice compared with that of CON mice, but was not changed in male mice (Figure 1B). To examine the effect of ERβ ablation on muscle, we measured the running performance and grip strength of the mice. There was no difference in running performance (Figure 1C). The absolute mean maximum strength was slightly decreased only in female mKO mice compared with CON mice (Figure 1D), while the relative strength per body weight was not different between mKO and CON mice (Figure 1E). Muscle weight and cross-sectional area (CSA) of tibialis anterior (TA) muscles were both significantly decreased in female mKO mice (Figures 1F and 1G). Because estrogen insufficiency in ovariectomized mice has been shown to influence muscle fiber types in TA muscle (Kitajima and Ono, 2016), we analyzed the fiber-type distribution. The ratio of each fiber type (IIa, IIx, and IIb) in female mKO mice was almost similar to the ratios in CON mice (Figure 1H). We also confirmed that no significant metabolic defect was observed in female mKO mice by conducting the glucose tolerance test (Figures S1C and S1D). Quantitative PCR (qPCR) analysis for anabolic (*AR* and *Igf1*) and catabolic (*Atrogin-1* and *MuRF-1*) genes revealed no drastic differences in both muscles *in vivo* (Figure 1I). Muscle mass and CSA of myofibers were unaltered when inactivation of ERβ was induced by the oral consumption of DOX in drinking water beginning at a later time (20 weeks of age) in adult female mice (data not shown), suggesting that ERβ is important for postnatal muscle growth in adult mice, but not for maintenance of muscle mass.

ERβ Is Required for Muscle Regeneration in Female, but Not Male, Mice

We next examined whether stem cells in skeletal muscle also exhibit sex differences. Recent findings, including ours (Kitajima and Ono, 2016), indicate that satellite cell function is influenced by estrogens. To generate satellite cell-specific ERβ KO mice (scKO) with tamoxifen (TMX), we crossed *Esr2*$^{f/f}$ mice with *Pax7*$^{CreERT2/+}$ mice. TMX-treated *Esr2*$^{f/f}$ mice were used as CON. Following serial treatment with TMX for 5 days, muscle injury was induced by injection of $BaCl_2$. Histological analysis demonstrated that ERβ-inactivated female mice exhibited a remarkable

Figure 1. Loss of ERβ in Muscle Results in Reduced Muscle Mass in Female Mice

(A) Schedule of doxycycline (DOX) treatment in *ACTA1-rtTA;tet0-Cre;Esr2*$^{f/f}$ (mKO) mice for induction of muscle-specific ERβ ablation. *Esr2*$^{f/f}$ mice were used as a control (CON).

(B) Body weight (n = 3–9 mice, each group).

(C) Endurance running performance (n = 5–6 mice, each group).

(D) Limb muscle force generation (n = 7–10 mice, each group).

(E) Limb muscle force generation normalized by body weight (n = 7–10, each group).

(F) Tibialis anterior (TA) muscle weight normalized by body weight (n = 5–6 mice, each group).

(G) Representative immunohistochemical images for laminin in TA muscles of cryosections. Cross-sectional area (CSA) in TA muscle was quantified (n = 7–8 mice, each group).

(H) Representative immunohistochemical images of the fiber-type composition (IIa, IIx, and IIx). Proportion of fiber types is shown (n = 4–5 mice, each group).

(I) qPCR analysis for the expression of anabolic and catabolic genes in TA muscle (n = 5–6 mice, each group).

Data represent means ± standard error of the mean. *p < 0.05; **p < 0.01; n.s., not significant. Student's t test.

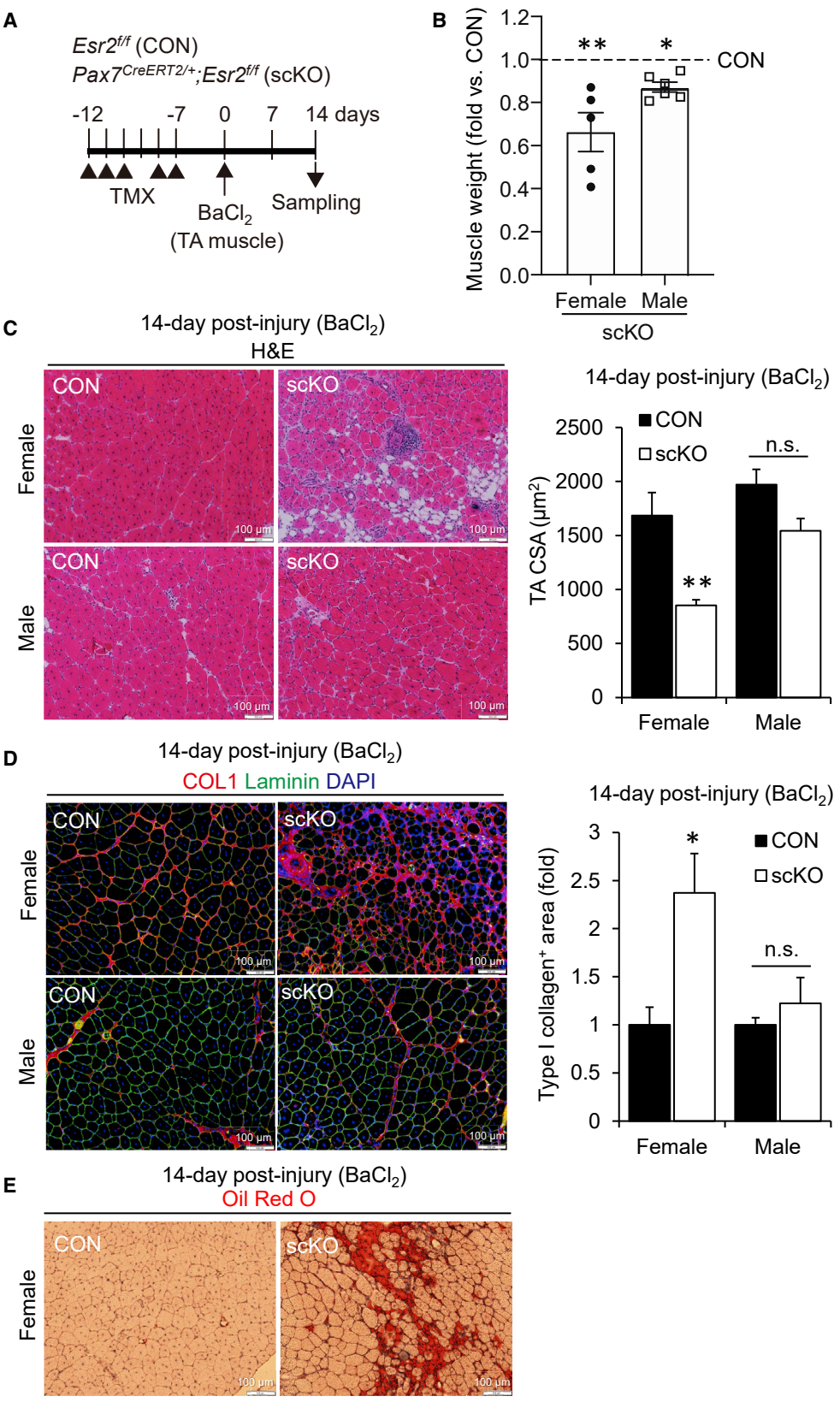

(legend on next page)

reduction in muscle weight (Figure 2B), compared with CON mice at 14 days following injury (Figure 2A). Although male scKO mice showed a slight reduction of muscle weight compared with male CON mice, female scKO mice were more severely affected by ERβ inactivation in satellite cells (Figure 2B). Importantly, CSA analysis of damaged muscles showed that muscle regeneration was remarkably perturbed in female scKO mice, but not in male scKO mice (Figure 2C). Pronounced accumulations of type I collagen (fibrotic tissue) (Figure 2D) and intramuscular adipose tissue as stained with oil red O (Figure 2E) were evident only in female scKO mice. To further investigate whether estrogen signaling is mediated through ERβ in satellite cells during muscle regeneration, estrogen insufficiency was induced by ovariectomized CON and scKO mice. Twenty-eight days post OVX, muscle injury was induced by injection of $BaCl_2$. Importantly, OVX-induced estrogen insufficiency did not further exacerbate the reduced CSA in scKO mice (Figures S1E–S1H). Altogether, these results suggest that female estrogens regulate the function of satellite cells through ERβ during muscle regeneration.

Inactivation of ERβ Decreases Proliferative Capacity of Satellite Cells

To investigate the mechanisms underlying the defect of muscle regeneration in female scKO mice, we isolated individual myofibers from the extensor digitorum longus (EDL) muscle of $Pax7^{CreERT2/+}$;$Esr2^{f/f}$ mice and analyzed satellite cells associated with myofibers. The number of satellite cells per myofiber was unchanged in both female and male scKO mice, compared with CON mice (Figure 3A). We examined the expression levels of ERα and ERβ mRNA in proliferating satellite cells in growth medium (GM) and the differentiating myotubes in differentiation medium (DM). qPCR analysis revealed that the expression of ERα was unaltered between GM and DM. In contrast, ERβ expression was relatively downregulated in DM compared with that in GM (Figure S2A), suggesting that ERβ is involved in satellite cell proliferation. Because estrogen deficiency in ovariectomized mice impairs the proliferation ability in satellite cells (Kitajima and Ono, 2016), we next analyzed this ability in satellite cells in the absence of ERβ. Satellite cells from male and female CON mice efficiently expanded, while satellite cells from male and female scKO mice failed to proliferate in the GM culture conditions (Figure 3B). Corresponding to these results, the presence of small interfering RNA (siRNA) against ERβ resulted in a marked decrease in the number of satellite cells compared with siCON (scrambled siRNA) (Figure 3C). Furthermore, treatment with a selective antagonist of ERβ, 4-(2-phenyl-5,7 bis(trifluoromethyl)- pyrazolo[1,5-a] pyrimidin-3-yl)-phenol (PHTPP), also confirmed the attenuation of the number of satellite cells in a dose-dependent manner (Figure S2B).

To next examine the effect of ERβ inactivation on the fate decision of satellite cells, we isolated satellite cells associated with individual myofibers from EDL and cultured them in floating conditions as previously described (Ono et al., 2011). In this culture model, three different populations are observed 3 days after plating based on immunostaining for PAX7 and MYOD. $PAX7^{+}MYOD^{+}$ cells are the activated/proliferative cells, $PAX7^{+}MYOD^{-}$ cells are the cells that self-renew to return to a quiescent-like state, and $PAX7^{-}MYOD^{+}$ cells are the cells that commit to differentiation. Although the total number of satellite cells was reduced, the proportion in each population was not different between scKO and CON mice (Figure 3D). These results suggest that ERβ regulates the proliferation of satellite cells after activation *in vitro*, but does not influence the satellite cell fate decision.

Loss of ERβ Causes a Defect in S-Phase Entry of the Cell Cycle

To further characterize the proliferation defect observed in ERβ-deleted satellite cells in culture (Figure 3), we isolated satellite cells from EDL muscle of $Pax7^{CreERT2/+}$;$Esr2^{f/f}$ mice and treated them with 4OH-TMX (scKO) to induce inactivation of ERβ *in vitro* (Figures 4A, 4B, and S1B). qPCR analysis showed that the gene expression of CyclinA2 (*Ccna2*), which is upregulated in the late G1-phase of the cell cycle, was significantly decreased in scKO cells (Figure 4B) and siEsr2-mediated knockdown cells (Figure S4A), compared with those of the corresponding controls. In contrast, expression of *p21*, a negative regulator of the cell cycle, was increased in scKO cells (Figure 4B). Microscopic analysis showed that the population of 5-ethynyl-2′-deoxyuridine (EdU)-positive

Figure 2. Loss of ERβ in Satellite Cells Impairs Muscle Regeneration

(A) Tamoxifen (TMX) was injected intraperitoneally five times into $Esr2^{f/f}$ (CON) mice and $Pax7^{CreERT2/+}$;$Esr2^{f/f}$ (scKO) mice. Mice were sacrificed at 14 days following $BaCl_2$ injection into TA muscle.

(B) TA muscle weight at 14 days post $BaCl_2$ injection (n = 5–6 mice, each group).

(C) H&E staining of TA muscle cross-sections at 14 days post $BaCl_2$ injection. The CSA was quantified (n = 3–4 mice, each group).

(D) Representative immunohistochemical images for collagen I (red) and laminin (green). Collagen I was used to quantify the area (n = 4 mice, each group).

(E) Representative oil red staining images for regenerating muscle of female mice.

Data represent means ± standard error of the mean. *p < 0.05; **p < 0.01; n.s., not significant. Student's t test.

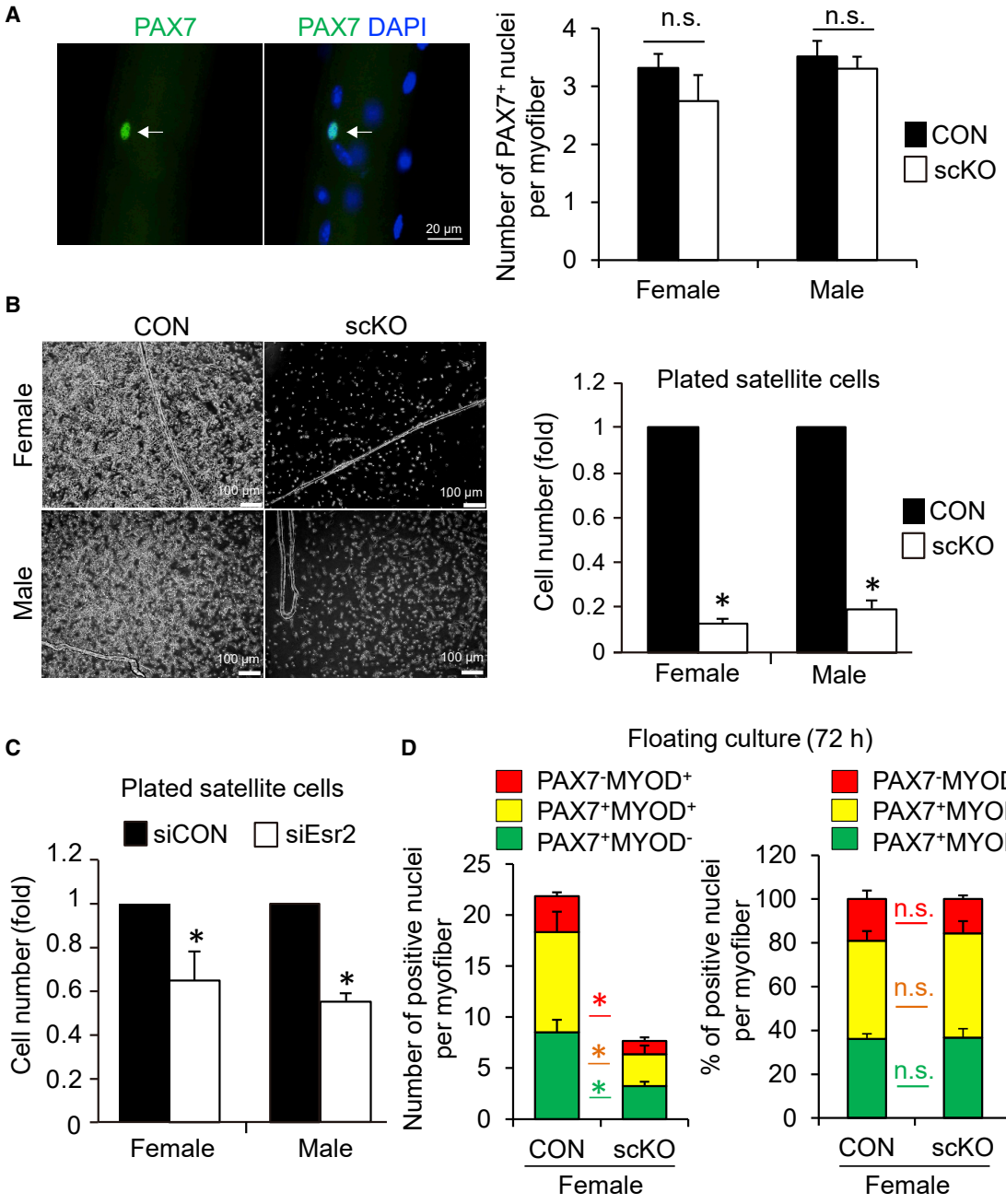

Figure 3. ERβ Is Essential for Satellite Cell Expansion *In Vitro*

(A) Immunofluorescence for PAX7 on myofibers freshly isolated from CON and scKO mice. The number of PAX7$^+$ satellite cells was quantified (n = 3–4 mice, each group).

(B) Representative microscopic images of primary cultured satellite cells isolated from CON or scKO mouse EDL muscles. Cells were maintained in growth medium for 6 days and the number of cells were quantified (n = 6 mice, each group).

(C) Primary cultured satellite cells were transfected with siRNA against Esr2 (siEsr2). Scramble control siRNA was used as control (siCON). The number of cells were quantified (n = 4 mice, each group).

(D) Individual myofibers associated with satellite cells were isolated from EDL muscle and cultured in plating medium for 72 h in floating conditions. Myofibers were fixed and immunostained for PAX7 and MYOD. The absolute number (left) or proportion (right) of PAX7 and/or MYOD positive cells per myofiber was quantified (n = 3–4 mice, each group).

Data represent means ± standard error of the mean. *p < 0.05; n.s., not significant. Student's t test.

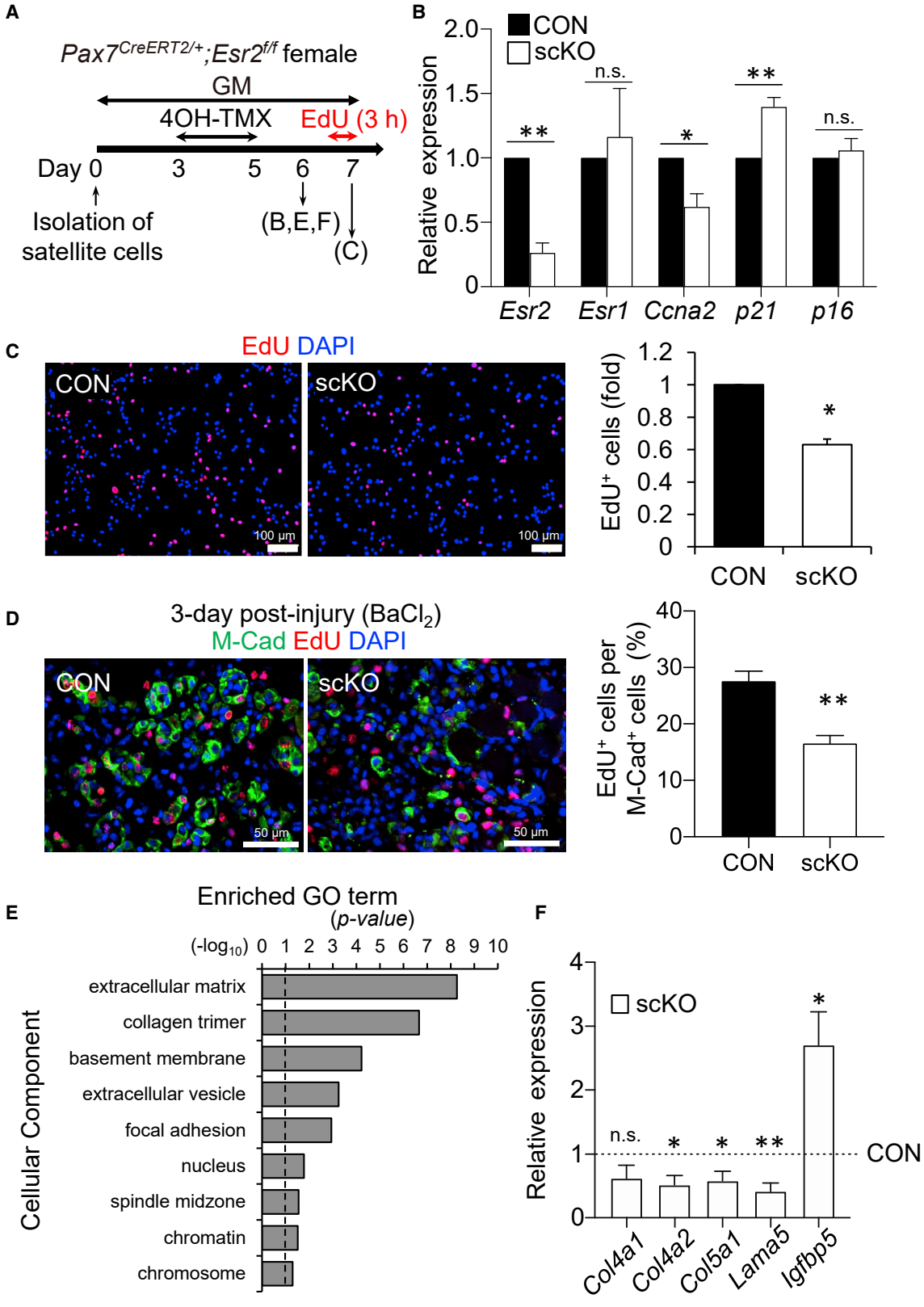

(legend on next page)

proliferating cells was decreased in scKO cells *in vitro* and *in vivo* (Figures 4C and 4D) and siRNA-mediated ERβ knocked down cells *in vitro* (Figures S4B and S4C), whereas myogenesis was not impaired by ERβ-inactivation (Figures S3A–S3D). Because β-Gal staining was not detected in scKO cells (data not shown) and p16 gene expression was unchanged between CON and scKO cells (Figure 4B), ERβ inactivation does not seem to induce cellular senescence. Cleaved caspase-3, an apoptosis marker, was remarkably increased in scKO cells or ERβ knocked down cells (Figures S3E, S3F, S4D, and S4E).

Finally, we performed RNA-sequencing analysis on activated satellite cells lacking ERβ. Gene ontology analysis revealed that the enriched categories in scKO female mice relative to CON mice were mostly gene sets related to the extracellular matrix, collagen trimer, basement membrane, extracellular vesicle, focal adhesion, nucleus, spindle midzone, chromatin, and chromosome (Figure 4E). qPCR further confirmed that extracellular matrix-related genes (*Col4a1*, *Col4a2*, *Col5a1*, *Lama5*), which are associated with cell proliferation (Thomas et al., 2015), were modestly downregulated. The Igfbp5 gene, which is involved in cellular senescence (Soriano-Arroquia et al., 2016), was upregulated in scKO cells (Figure 4F), although treatment with recombinant IGFBP5 protein did not affect population expansion of satellite cells in culture (data not shown). Taken together, our data suggest that ERβ controls the optimal population expansion by regulating transcriptions of niche-associated genes and cell-cycle-associated genes in satellite cells.

DISCUSSION

Although ERβ is expressed in both male and female muscle tissues, we observed that male mKO mice did not display obvious phenotypes in muscle mass and strength. These results suggest that ERβ is dispensable to maintain the muscle function in male mice, corresponding to very low levels of estrogens in the blood of male mice. ERβ inactivation by the consumption of DOX in drinking water starting at 6 weeks of age resulted in the decreased CSA of the TA muscle in female mice. However, it is unlikely that ERβ is essential for maintenance of adult muscle of female mice because ERβ ablation did not influence muscle mass and function when its inactivation was induced by DOX later in life (20 weeks) in female mice (data not shown), suggesting that ERβ is more important for growth of muscles rather than maintenance of their mass. In support of this result, we further confirmed that atrophy-related genes were unchanged in ERβ muscles. With these results, we think that ERβ is involved in female-specific signaling that is important for the regulation of postnatal muscle growth, rather than preventing muscle atrophy, in young female mice. In addition, ERβ inactivation in muscles does not affect the whole-body metabolism or muscle fiber composition. Considering that ERα controls muscle metabolic function in female mice (Ribas et al., 2016; Schweisgut et al., 2017), ERβ and ERα may have distinct roles in skeletal muscles. While we provide evidence that ERβ influences postnatal muscle growth, the downstream pathway of ERβ as well as its transcriptional targets remain unknown. Further studies will be required to distinguish the function of the estrogen-ERβ signaling pathways in muscle between postnatal muscle growth and maintenance of adult muscle in female mice.

We previously showed that estrogen insufficiency results in a marked defect in muscle regeneration following cardiotoxin injection in OVX female mice (Kitajima and Ono, 2016). This regenerative failure is probably due to the reduced population expansion of satellite cells in female mice (Kitajima and Ono, 2016). In the present study, we asked whether ERβ expressed in satellite cells is involved in muscle regeneration. *Ccna2*, a cell-cycle regulator, is known to be one of the estrogen-target genes (Vendrell et al., 2004). We found that ERβ deletion resulted in a decrease in expression of *Ccna2* as well as an impairment of proliferation in satellite cells. We also showed that loss of ERβ increased apoptosis in satellite cells. Indeed, we speculate that a lower level of *Ccna2* and activation of the apoptosis pathway may be involved in the defective population expansion of ERβ-inactivated satellite cells. Furthermore, RNA-sequencing analysis highlighted that the expression of niche-related genes was remarkably altered by ERβ inactivation. Thus, abnormal niche may influence the cellular function of ERβ--deleted satellite cells, in support of recent studies (Baghdadi

Figure 4. ERβ Deletion Suppresses Cell-Cycle Entry in Satellite Cells

(A) Schedule of 4-hydroxy tamoxifen (4OH-TMX) treatment in cultured satellite cells isolated from *Pax7*$^{CreERT2/+}$;*Esr2*$^{f/f}$ mice.

(B) qPCR analysis of the expression of *Esr2*, *Esr1*, *Ccna2*, *p21*, and *p16* in CON and scKO cells (n = 3 mice, each group).

(C) EdU staining of primary satellite cells. EdU^{+} cells per DAPI + cells were quantified (n = 4 mice, each group).

(D) EdU staining of muscle cross-section at day 3 post injury. EdU^{+} cells per M-Cadherin^{+} satellite cells were quantified (n = 3–5 mice, each group).

(E) Gene ontology analysis of RNA-sequencing data was performed (scKO versus CON) (n = 3 mice, each group).

(F) qPCR analysis for the expression of extracellular matrix-related genes (*Col4a1*, *Col4a2*, *Col5a1*, *Lama5*) and *Igfbp5* (n = 4–5 mice, each group).

Data represent means ± standard error of the mean. *p < 0.05; **p < 0.01; n.s., not significant. Student's t test.

et al., 2018; Urciuolo et al., 2013). However, it remains to be investigated whether ERβ signaling directly regulates transcription for the niche-related genes.

We found a significant impairment in progenitor population expansion of satellite cells of male ERβ scKO mice as well as females in culture *in vitro*. These results are not consistent with *in vivo* observations that male ERβ-deleted mice show a mild or no defect in muscle regeneration *in vivo*. This discrepancy may be explained by an environment where satellite cells expand. Because serum estradiol levels in blood are high in females but very low in males *in vivo*, the impact of ERβ inactivation was more prominent in females compared with males even though the level of the ERβ expression between males and females is almost identical. In our *in vitro* experiments, we used serum-rich culture medium (30% fetal bovine serum and 1% chick embryonic extract in DMEM) that contained estradiol. The DMEM solution also contains phenol red, which exerts estrogenic activity as a selective estrogen receptor modulator (Berthois et al., 1986; Welshons et al., 1988). Thus, our results suggest that the estradiol-rich culture conditions permit population expansion of both female and male mouse-derived satellite cells *in vitro* through the estrogen-ERβ signaling pathway. However, it remains unclear how male mice regenerate muscle in an estrogen-ERβ independent mechanism *in vivo*.

In conclusion, our findings provide evidence that the estrogen-ERβ pathway is a female-specific regulatory mechanism controlling skeletal muscle mass and strength, as well as expansion of satellite cells in muscle regeneration. Therefore, sex-specific therapeutic strategies will be required for ameliorating age-related muscle loss and muscle diseases. Targeting ERβ or enhancing estrogen-ERβ signaling could be a therapeutic option in women.

EXPERIMENTAL PROCEDURES

Animals

The experimental procedures were approved by the Ethical Committee for Animal Care and Use of Nagasaki University (no. 1203190970) and Kumamoto University (A30-098). ERβ-floxed (Antal et al., 2008) mice, which were kindly provided by Prof. Pierre Chambon, were crossed with *ACTA1-rtTA;tetO-Cre* mice (Rao and Monks, 2009) and $Pax7^{CreERT2}$ mice (Lepper and Fan, 2012) to generate *ACTA1-rtTA;tetO-Cre;*$ERβ^{f/f}$ and $Pax7^{CreERT2/+}$;$ERβ^{f/f}$ (scKO) mice, respectively. To delete ERβ in skeletal muscle, the rtTA/TRE-driven expression of Cre recombinase was induced by providing mice with drinking of water containing 2 mg/mL DOX and 5% sucrose for 3 weeks. To delete ERβ in satellite cells, TMX dissolved in corn oil (5 μL/g, 20 mg/mL) was injected intraperitoneally five times as previously described (Ono et al., 2015). To induce muscle injury, 50 μL of $BaCl_2$ was injected intramuscularly into the TA muscle of anesthetized mice using a Hamilton syringe. Regenerating muscles were isolated at day 14 following $BaCl_2$ injection. Transverse muscle sections were cut using a cryostat and immunostained.

Statistical Analysis

Significant differences between datasets were determined using the Student t test, and $p < 0.05$ indicates statistically significant differences. All data represent the mean ± standard error of the mean.

Data and Code Availability

The RNA-sequencing data have been deposited under accession number GEO: GSE135837.

SUPPLEMENTAL INFORMATION

Supplemental Information can be found online at https://doi.org/10.1016/j.stemcr.2020.07.017.

AUTHOR CONTRIBUTIONS

D.S. and R.F. conceived and designed the study and performed experiments, collected data, and wrote the manuscript. Y.K. and K.N. performed experiments. Y.I. provided expertise for the RNA-sequencing data. Y.O. conceived and designed the study, assembled the input data, and wrote the manuscript. All authors discussed the results and implications and commented on the manuscript. D.S. and R.F. contributed equally to the study.

ACKNOWLEDGMENTS

We thank Yumiko Takemoto for technical assistance, Koichi Ikuta for sending materials, and all lab members for technical support and useful discussion. This work was supported by the Japan Agency for Medical Research and Development (AMED, 18ek0109383h0001 and 19bm0704036h0001), and the Grant-in-Aid for Scientific Research KAKENHI (18H03193, and 18K19749). R.F. is funded by a JSPS Overseas Research Fellowship, the Uehara Memorial Foundation, the Kanzawa Medical Research Foundation, and the leading initiative for Excellent Young Researchers, MEXT, Japan. K.N. is supported by a JSPS Research Fellowship. This work was also supported, in part, by the Meiji Yasuda Life Foundation of Health and Welfare and the Takeda Science Foundation.

Received: August 21, 2019
Revised: July 22, 2020
Accepted: July 22, 2020
Published: August 20, 2020

REFERENCES

Antal, M.C., Krust, A., Chambon, P., and Mark, M. (2008). Sterility and absence of histopathological defects in nonreproductive organs of a mouse ERbeta-null mutant. Proc. Natl. Acad. Sci. U S A *105*, 2433–2438.

Baghdadi, M.B., Castel, D., Machado, L., Fukada, S.I., Birk, D.E., Relaix, F., Tajbakhsh, S., and Mourikis, P. (2018). Reciprocal signalling by Notch-Collagen V-CALCR retains muscle stem cells in their niche. Nature *557*, 714–718.

Baltgalvis, K.A., Greising, S.M., Warren, G.L., and Lowe, D.A. (2010). Estrogen regulates estrogen receptors and antioxidant gene expression in mouse skeletal muscle. PLoS One *5*, e10164.

Berthois, Y., Katzenellenbogen, J.A., and Katzenellenbogen, B.S. (1986). Phenol red in tissue culture media is a weak estrogen: implications concerning the study of estrogen-responsive cells in culture. Proc Natl Acad Sci U S A *83*, 2496–2500.

Brack, A.S., and Rando, T.A. (2012). Tissue-specific stem cells: lessons from the skeletal muscle satellite cell. Cell Stem Cell *10*, 504–514.

Collins, B.C., Arpke, R.W., Larson, A.A., Baumann, C.W., Xie, N., Cabelka, C.A., Nash, N.L., Juppi, H.K., Laakkonen, E.K., Sipila, S., et al. (2019). Estrogen regulates the satellite cell compartment in females. Cell Rep. *28*, 368–381.e6.

Diel, P. (2014). The role of the estrogen receptor in skeletal muscle mass homeostasis and regeneration. Acta Physiol. (Oxf.) *212*, 14–16.

Enns, D.L., and Tiidus, P.M. (2008). Estrogen influences satellite cell activation and proliferation following downhill running in rats. J. Appl. Physiol. *104*, 347–353.

Hamilton, K.J., Hewitt, S.C., Arao, Y., and Korach, K.S. (2017). Estrogen hormone biology. Curr. Top. Dev. Biol. *125*, 109–146.

Kim, J.H., Han, G.C., Seo, J.Y., Park, I., Park, W., Jeong, H.W., Lee, S.H., Bae, S.H., Seong, J., Yum, M.K., et al. (2016). Sex hormones establish a reserve pool of adult muscle stem cells. Nat. Cell Biol. *18*, 930–940.

Kitajima, Y., and Ono, Y. (2016). Estrogens maintain skeletal muscle and satellite cell functions. J. Endocrinol. *229*, 267–275.

Kitajima, Y., Ogawa, S., Egusa, S., and Ono, Y. (2017). Soymilk improves muscle weakness in young ovariectomized female mice. Nutrients *9*, 834.

Kuang, S., and Rudnicki, M.A. (2008). The emerging biology of satellite cells and their therapeutic potential. Trends Mol. Med. *14*, 82–91.

Lepper, C., and Fan, C.M. (2012). Generating tamoxifen-inducible Cre alleles to investigate myogenesis in mice. Methods Mol. Biol. *798*, 297–308.

Mauro, A. (1961). Satellite cell of skeletal muscle fibers. J. Biophys. Biochem. Cytol. *9*, 493–495.

McClung, J.M., Davis, J.M., Wilson, M.A., Goldsmith, E.C., and Carson, J.A. (2006). Estrogen status and skeletal muscle recovery from disuse atrophy. J. Appl. Physiol. *100*, 2012–2023.

Ogawa, M., Kitakaze, T., Harada, N., and Yamaji, R. (2015). Female-specific regulation of skeletal muscle mass by USP19 in young mice. J. Endocrinol. *225*, 135–145.

Ono, Y., Calhabeu, F., Morgan, J.E., Katagiri, T., Amthor, H., and Zammit, P.S. (2011). BMP signalling permits population expansion by preventing premature myogenic differentiation in muscle satellite cells. Cell Death Differ. *18*, 222–234.

Ono, Y., Urata, Y., Goto, S., Nakagawa, S., Humbert, P.O., Li, T.S., and Zammit, P.S. (2015). Muscle stem cell fate is controlled by the cell-polarity protein Scrib. Cell Rep. *10*, 1135–1148.

Rao, P., and Monks, D.A. (2009). A tetracycline-inducible and skeletal muscle-specific Cre recombinase transgenic mouse. Dev. Neurobiol. *69*, 401–406.

Relaix, F., and Zammit, P.S. (2012). Satellite cells are essential for skeletal muscle regeneration: the cell on the edge returns centre stage. Development *139*, 2845–2856.

Ribas, V., Drew, B.G., Zhou, Z., Phun, J., Kalajian, N.Y., Soleymani, T., Daraei, P., Widjaja, K., Wanagat, J., de Aguiar Vallim, T.Q., et al. (2016). Skeletal muscle action of estrogen receptor alpha is critical for the maintenance of mitochondrial function and metabolic homeostasis in females. Sci. Transl. Med. *8*, 334ra354.

Schweisgut, J., Schutt, C., Wust, S., Wietelmann, A., Ghesquiere, B., Carmeliet, P., Drose, S., Korach, K.S., Braun, T., and Boettger, T. (2017). Sex-specific, reciprocal regulation of ERalpha and miR-22 controls muscle lipid metabolism in male mice. EMBO J. *36*, 1199–1214.

Seko, D., Ogawa, S., Li, T.S., Taimura, A., and Ono, Y. (2016). muCrystallin controls muscle function through thyroid hormone action. FASEB J. *30*, 1733–1740.

Shimizu-Motohashi, Y., Asakura, Y., Motohashi, N., Belur, N.R., Baumrucker, M.G., and Asakura, A. (2015). Pregnancy-induced amelioration of muscular dystrophy phenotype in mdx mice via muscle membrane stabilization effect of glucocorticoid. PLoS One *10*, e0120325.

Sinha-Hikim, I., Cornford, M., Gaytan, H., Lee, M.L., and Bhasin, S. (2006). Effects of testosterone supplementation on skeletal muscle fiber hypertrophy and satellite cells in community-dwelling older men. J. Clin. Endocr. Metab. *91*, 3024–3033.

Sipila, S., and Poutamo, J. (2003). Muscle performance, sex hormones and training in peri-menopausal and post-menopausal women. Scand. J. Med. Sci. Sports *13*, 19–25.

Sitnick, M., Foley, A.M., Brown, M., and Spangenburg, E.E. (2006). Ovariectomy prevents the recovery of atrophied gastrocnemius skeletal muscle mass. J. Appl. Physiol. *100*, 286–293.

Soriano-Arroquia, A., McCormick, R., Molloy, A.P., McArdle, A., and Goljanek-Whysall, K. (2016). Age-related changes in miR-143-3p:Igfbp5 interactions affect muscle regeneration. Aging Cell *15*, 361–369.

Thomas, K., Engler, A.J., and Meyer, G.A. (2015). Extracellular matrix regulation in the muscle satellite cell niche. Connect. Tissue Res. *56*, 1–8.

Tierney, M.T., and Sacco, A. (2016). Satellite cell heterogeneity in skeletal muscle homeostasis. Trends Cell Biol. *26*, 434–444.

Tiidus, P.M., Holden, D., Bombardier, E., Zajchowski, S., Enns, D., and Belcastro, A. (2001). Estrogen effect on post-exercise skeletal muscle neutrophil infiltration and calpain activity. Can. J. Physiol. Pharmacol. *79*, 400–406.

Urciuolo, A., Quarta, M., Morbidoni, V., Gattazzo, F., Molon, S., Grumati, P., Montemurro, F., Tedesco, F.S., Blaauw, B., Cossu, G., et al. (2013). Collagen VI regulates satellite cell self-renewal and muscle regeneration. Nat. Commun. *4*, 1964.

Velders, M., Schleipen, B., Fritzemeier, K.H., Zierau, O., and Diel, P. (2012). Selective estrogen receptor-beta activation stimulates skeletal muscle growth and regeneration. FASEB J. *26*, 1909–1920.

Vendrell, J.A., Magnino, F., Danis, E., Duchesne, M.J., Pinloche, S., Pons, M., Birnbaum, D., Nguyen, C., Theillet, C., and Cohen, P.A. (2004). Estrogen regulation in human breast cancer cells of new downstream gene targets involved in estrogen metabolism, cell proliferation and cell transformation. J. Mol. Endocrinol. *32*, 397–414.

Welshons, W.V., Wolf, M.F., Murphy, C.S., and Jordan, V.C. (1988). Estrogenic activity of phenol red. Mol Cell Endocrinol. *57*, 169–178.

Wiik, A., Ekman, M., Johansson, O., Jansson, E., and Esbjornsson, M. (2009). Expression of both oestrogen receptor alpha and beta in human skeletal muscle tissue. Histochem. Cell Biol. *131*, 181–189.

Stem Cell Reports, Volume *15*

Supplemental Information

Estrogen Receptor β Controls Muscle Growth and Regeneration in Young Female Mice

Daiki Seko, Ryo Fujita, Yuriko Kitajima, Kodai Nakamura, Yuuki Imai, and Yusuke Ono

Figure S1

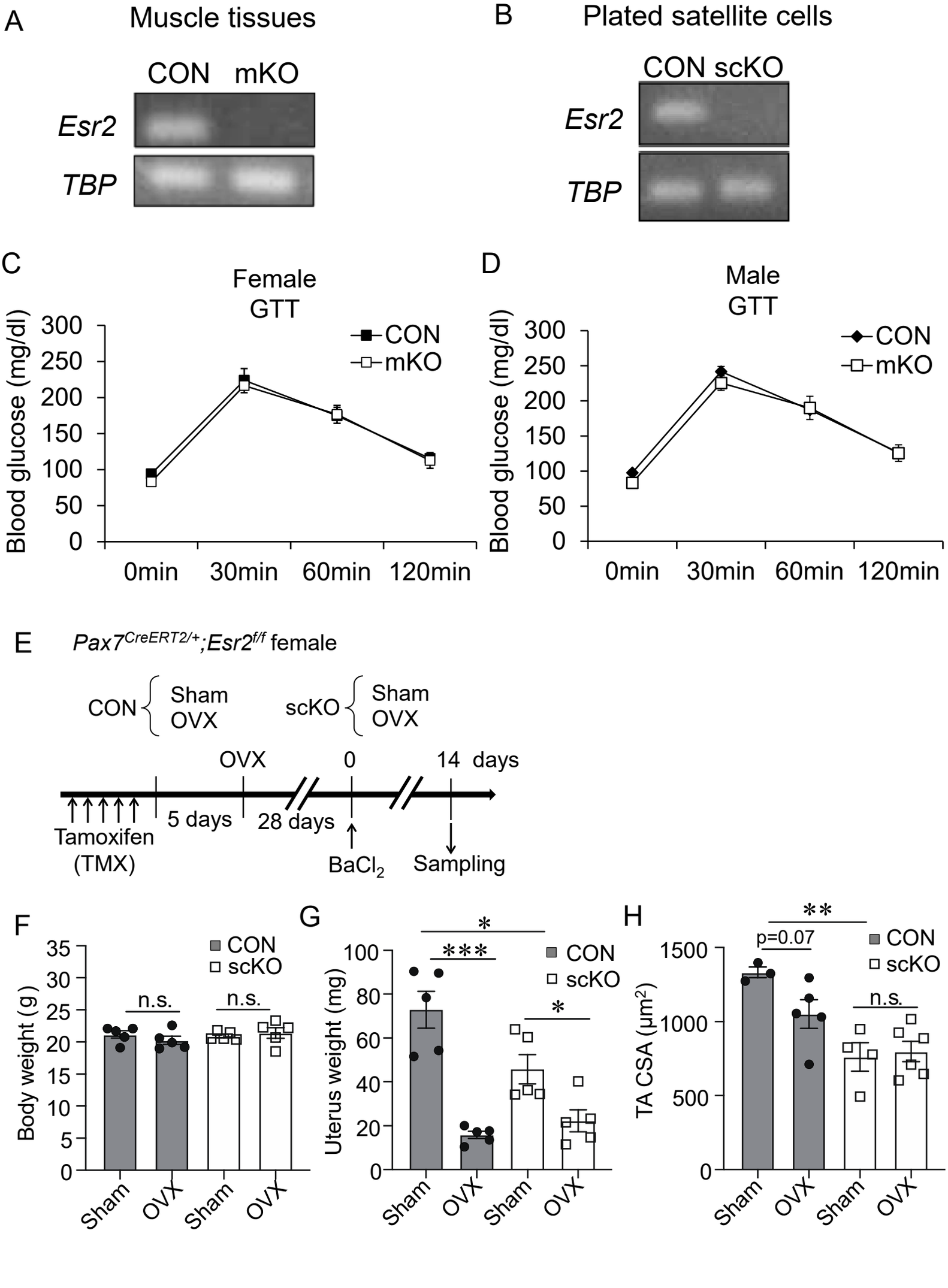
A
Muscle tissues
CON mKO
Esr2
TBP
B
Plated satellite cells
CON scKO
Esr2
TBP
C
Female GTT
Blood glucose (mg/dl)
CON
mKO
0min 30min 60min 120min
D
Male GTT
Blood glucose (mg/dl)
CON
mKO
0min 30min 60min 120min
E
Pax7CreERT2/+;Esr2f/f female
CON Sham OVX
scKO Sham OVX
OVX 0 14 days
5 days 28 days
Tamoxifen (TMX)
BaCl2
Sampling
F
Body weight (g)
CON scKO
n.s. n.s.
Sham OVX Sham OVX
G
Uterus weight (mg)
* *** *
CON scKO
Sham OVX Sham OVX
H
TA CSA (μm2)
** p=0.07 n.s.
CON scKO
Sham OVX Sham OVX

Figure S1. OVX does not further exacerbate the impaired muscle regeneration in ERβ scKO mice

(A-B) Representative images of RT-PCR products for *Esr2* in TA muscles (A) or satellite cells (B).

(C-D) Glucose metabolism is not altered in muscle-specific ERβ inactivated mice. (C) Glucose tolerance test was performed in female CON and mKO mice (CON, n=5 mice; mKO, n=5 mice). (D) Glucose tolerance test was performed in male CON and mKO mice (CON, n=3 mice; mKO, n=3 mice). Data represent means ± standard error of the mean. not significant. Student's t test.

(E-H) OVX-induced estrogen insufficiency does not further exacerbate the reduced myofiber sizes in ERβ scKO mice. (E) TMX was injected intraperitoneally into *Esr2*$^{f/f}$ (CON) mice and *Pax7*$^{CreERT2/+}$*;Esr2*$^{f/f}$ (scKO) mice. Mice were ovariectomized (OVX) for 28 days at day 5 following TMX injection and sacrificed at day 14 following $BaCl_2$ injection into TA muscle. (F) Body weight (Sham-CON, n=5 mice; OVX-CON, n=5 mice; Sham-CON, n=5 mice; OVX-scKO, n=6 mice). (G) Uterus weight (Sham-CON, n=5 mice; OVX-CON, n=5 mice; Sham-CON, n=5 mice; OVX-scKO, n=6 mice). (H) CSA of TA muscle (Sham-CON, n=3 mice; OVX-CON, n=5 mice; Sham-CON, n=4 mice; OVX-scKO, n=6 mice). Data represent means±standard error of the mean. *, p<.05; **, p<.01; ***, p<.001; n.s., not significant, one-way ANOVA followed by Bonferroni's multiple comparison tests.

Figure S2

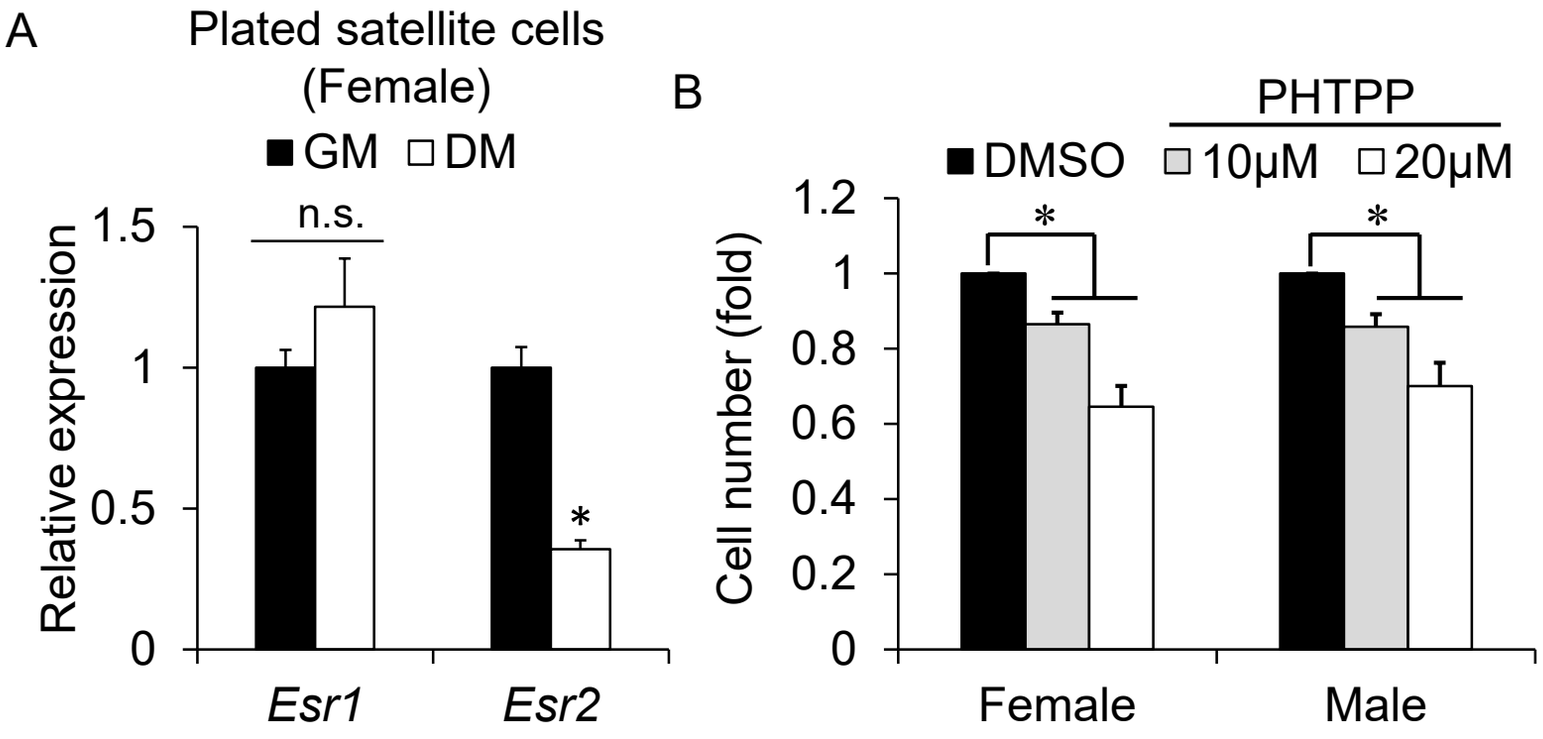

Figure S2. Satellite cell proliferation is attenuated by treatment with an ERβ selective antagonist

(A) Q-PCR analysis for the expression of *Esr2* and *Esr1* in primary satellite cells maintained in GM and DM culture conditions (n=3 mice, each group).

(B) The number of satellite cells treated with PHTTP, a selective antagonist of ERβ (n=3 mice, each group).

Data represent means ± standard error of the mean. *, p<.05; n.s., not significant. Student's t test.

Figure S3

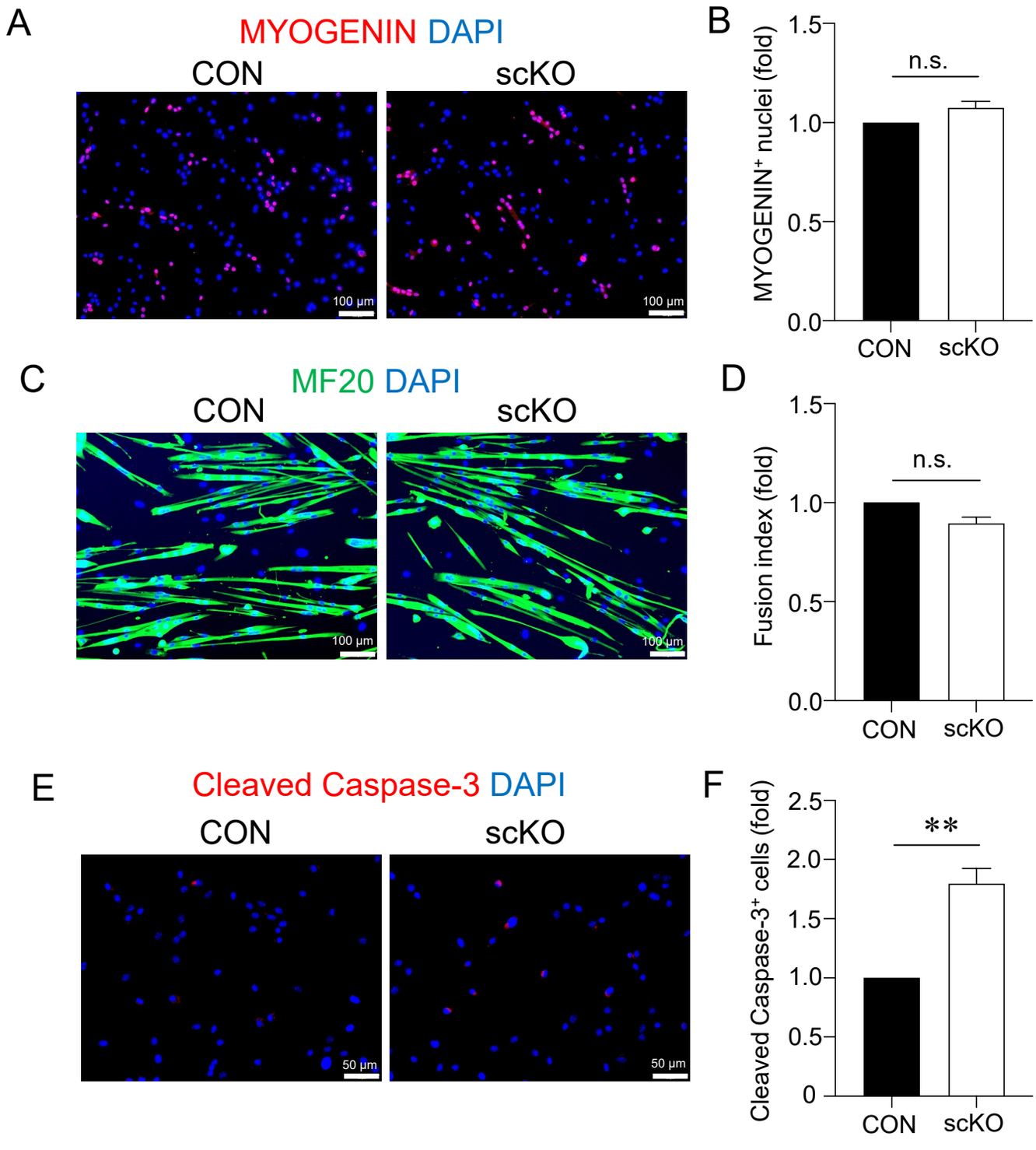

Figure S3. Effects of ERβ deletion on apoptosis and differentiation of satellite cells

(A-F) Satellite cells were isolated from *Pax7*$^{CreERT2/+}$*;Esr2*$^{f/f}$ mice and ERβ was inactivated by 4OH-TMX treatment as shown in Fig.4A.

(A-B) Immunofluorescence for MYOGENIN in ERβ-deleted satellite cells in GM. Representative images (A) and quantitative data for MYOGENIN$^+$ nuclei per DAPI$^+$ nuclei (B). n=3 mice, each group.

(C-D) Myogenic differentiation was induced in ERβ-deleted satellite cells in DM. (C) Representative images of immunofluorescence for MF20. (D) Myogenesis was evaluated by fusion index (the relative number of MF20$^+$ myotubes that contain more than 5 nuclei per MF20$^+$ nuclei). n=3 mice, each group.

(E-F) Immunofluorescence for cleaved Caspase-3 in ERβ-deleted satellite cells in GM. Representative images (E) and quantitative data for cleaved Caspase-3$^+$ nuclei per DAPI$^+$ nuclei (F). n=3 mice, each group.

Data represent means ± standard error of the mean. **, p<.01; n.s., not significant. Student's t test.

Figure S4

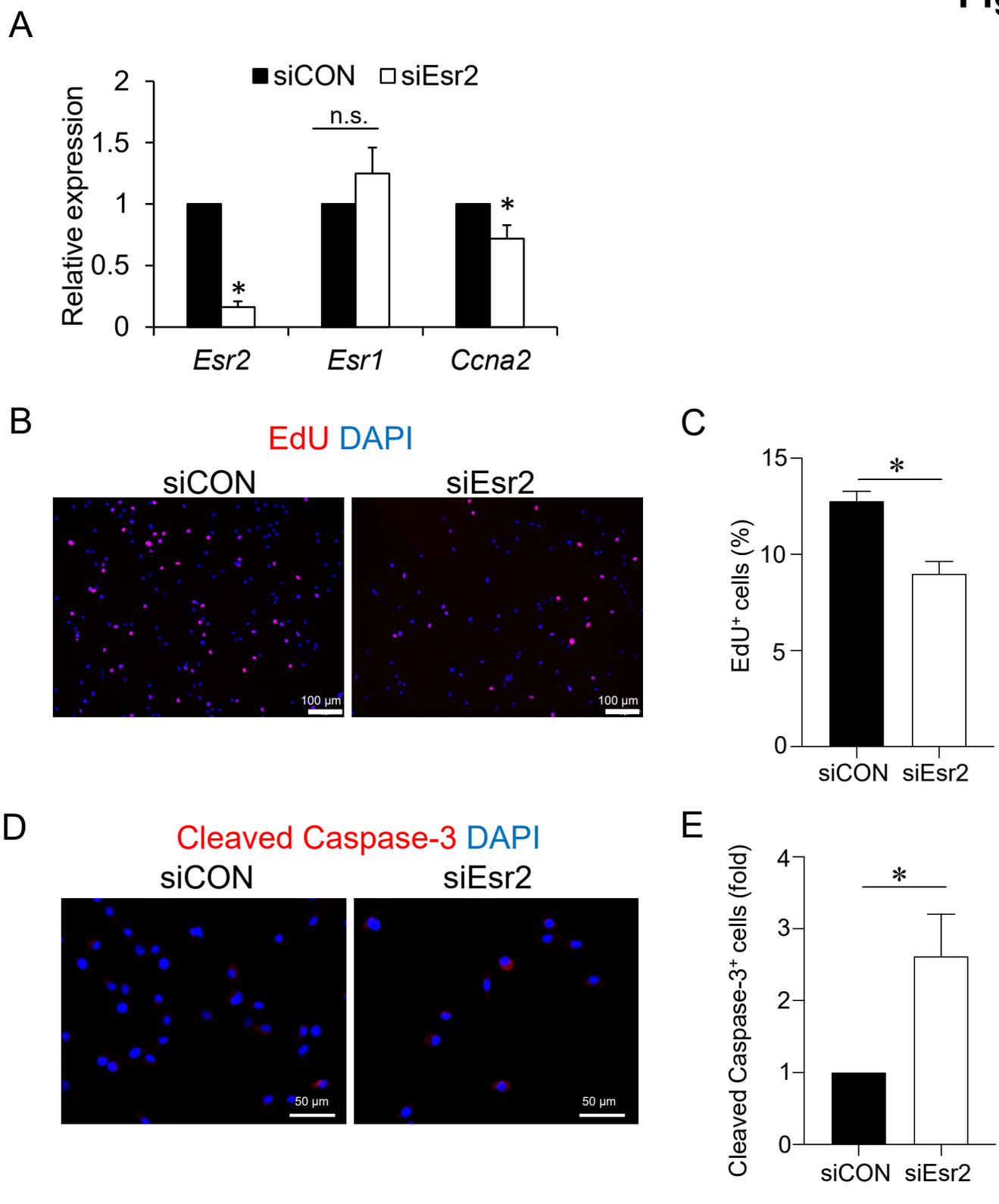

Figure S4. Knockdown of ERβ suppresses cell cycle entry and induces apoptosis in satellite cells

(A-E) Effects of siRNA-mediated knockdown of ERβ on satellite cells in culture.

(A) Q-PCR analysis for the expression of *Esr2*, *Esr1*, and *Ccna2* in siRNA-transfected satellite cells. n=3 mice, each group.

(B-C) EdU staining of satellite cells. Representative images (B) and quantitative data for EdU^+ nuclei per $DAPI^+$ nuclei (C). n=4 mice, each group.

(D-E) Immunofluorescence of cleaved $Caspase\text{-}3^+$ satellite cells. Representative images (D) and quantified data (E). n=3 mice, each group.

Data represent means ± standard error of the mean. *, $p<.05$; n.s., not significant. Student's t test.

Supplemental Experimental Procedures

Antibodies and reagents

Mouse anti-Type IIa myosin heavy chain (MyHC) (SC-71) and mouse anti-Type IIb MyHC (BF-F3) antibodies were obtained from Deutsche Sammlung von Mikroorganismen (Braunschweig, Germany). Mouse anti-myosin heavy chain (MF20) antibody was obtained from R&D Systems (Minneapolis, MN). Mouse anti-PAX7, mouse anti-MYOGENIN, and rabbit anti-MYOD antibodies were purchased from Santa Cruz Biotechnology (Santa Cruz, CA). Rat anti-laminin α2 antibody was obtained from Alexis (San Diego, CA, USA). Rabbit anti-M-Cadherin and rabbit anti-Cleaved Caspase-3 antibodies were purchased from Cell Signaling Technology (Beverly, MA). Goat anti-collagen Type I antibody was purchased from Southern Biotech (Birmingham, AL, USA). The mounting medium containing 4′,6-diamidino-2-phenylindole for nuclear staining and a Mouse On Mouse (M.O.M.) kit were purchased from Vector Laboratories (Burlingame, CA, USA). Tamoxifen (TMX) and 4-hydroxy TMX (4OH-TMX) were purchased from Sigma-Aldrich (St. Louis, MO, USA). A selective antagonist of ERβ, 4-(2-phenyl-5,7 bis(trifluoromethyl)-pyrazolo[1,5-a] pyrimidin-3-yl)-phenol

16 (PHTPP), was purchased from Sigma-Aldrich. The Click-iT ™ EdU Cell Proliferation Kit was
17 purchased from Thermo Fisher Scientific (Waltham, MA).
18
19 **Muscle functional tests i*n vivo***
20 Mice 10- to 13-weeks of age were subjected to a low-intensity, run-to-exhaustion protocol on
21 a motorized treadmill as previously described (Fujita et al., 2018). The mice were familiarized
22 with the treadmill (Muromachi Kikai, Tokyo, Japan) for 10 min at 10 m/min for 2 consecutive
23 days. The next day, each mouse were run at 10 m/min for 30 min, 11 m/min for 15 min, and
24 12 m/min for 15 min with a 15° incline. Finally, the speed was incrementally increased by 1
25 m/min every 10 min until the mouse exhibited exhaustion. The endpoint was achieved when
26 the mouse sat on the shock grid at the back of the treadmill for longer than 5 s.
27 Whole-limb grip strength was measured using a Grip Strength Meter for mice
28 (Columbus Instruments, Columbus, OH, USA) as previously described (Fujita et al., 2018).
29 Peak tension (in newtons) was recorded when the mouse released its grip. Two sets of 10
30 successive measurements were performed for each mouse and the mean maximum strength
31 in each set of experiments was used for data analysis.

Glucose tolerance test

A glucose tolerance test was performed by intraperitoneal glucose injection (1 g/kg body weight) after overnight food withdrawal (16 h). Blood-glucose concentrations were measured using an Accu-Chek meter (Roche, Basel, Switzerland) before (0 min) and 30, 60, and 120 min after glucose injection.

Myofiber and satellite cell isolation and culture

EDL muscles were isolated and digested with type I collagenase as previously described (Ono et al., 2015). Satellite cells were obtained from isolated myofibers and cultured in GM (Dulbecco's modified Eagle's medium (DMEM) supplemented with 30% fetal bovine serum, 1% chicken-embryo extract, 10 ng/mL basic fibroblast growth factor, and 1% penicillin-streptomycin) at 37°C in a 5% CO_2 atmosphere. Myogenic differentiation was induced in DM (DMEM supplemented with 5% horse serum and 1% penicillin-streptomycin) at 37°C in a 5% CO_2 atmosphere. For floating culture, isolated myofibers associated with satellite cells were

47 cultured in plating medium (PM; DMEM supplemented with 10% horse serum, 0.5% chick
48 embryo extract, and 1% penicillin-streptomycin) at 37°C in a 5% CO_2 atmosphere.
49
50 **Immunostaining**
51 Immunocytochemistry of satellite cells associated with myofibers was performed as
52 previously described (Ono et al., 2015). Samples were fixed with 4% paraformaldehyde,
53 blocked/permeabilized with phosphate-buffered saline containing 0.3% Triton X100 and 5%
54 goat or porcine serum for 20 min at room temperature, and incubated with primary antibodies
55 at 4°C overnight. TA muscle tissues were immediately frozen in 2-methylbutane cooled in
56 liquid nitrogen and stored at −80°C before being cryosectioned. Hematoxylin and eosin
57 (H&E) staining and Oil Red O staining were performed as previously described (Fujita et al.,
58 2018). Frozen cross-sections of TA muscle were fixed with 4% paraformaldehyde, blocked
59 with M.O.M., and incubated with primary antibodies at 4°C overnight. All immunostaining
60 samples were visualized using appropriate species-specific Alexa Fluor 488 and/or 568
61 fluorescence-conjugated secondary antibodies (Thermo Fisher Scientific, Waltham, MA).
62 Samples were viewed on an Olympus microscope IX83 (Olympus, Tokyo, Japan) or a

CellInsight CX5 (Thermo Fisher Scientific). Digital images were acquired and quantified with a DP80 camera using cellSens software (Olympus). Images were optimized globally and assembled into figures using Adobe Photoshop.

siRNA transfection

Transfection of siRNA was performed as previously described (Ono et al., 2011). Isolated satellite cells were seeded in six-well plates and transfected with siRNA at 30-40% confluence. MISSION siRNA (Sigma-Aldrich) were diluted in OptiMEM (Thermo Fisher Scientific) to 2-10 pmol per well and incubated with RNAiMAX (Thermo Fisher Scientific) diluted in OptiMEM according to the manufacturer's instructions. The following siRNA sequences were used: Esr2 siRNA (SASI_Mm01_00185612 (siRNA #1); SASI_Mm02_00317914 (siRNA #2). A control siRNA sequence selected by Sigma-Aldrich was used.

Q-PCR

Total RNA was extracted from cultured satellite cells or muscle tissues using an RNAeasy Kit (Qiagen, Hilden, Germany) or an ISOGEN II (Nippon Gene, Tokyo, Japan), respectively.

cDNA was prepared with a ReverTra Ace kit with genomic DNA remover (Toyobo, Tokyo, Japan). Q-PCR was performed using a THUNDERBIRD SYBR qPCR mix and CFX96 Touch real-time PCR detection system (Bio Rad, Tokyo, Japan). Primer sequences were as follows: TATA box binding protein (TBP) as a normalizer (F 5'-CAGATGTGCGTCAGGCGTTC-3' and R 5'-TAGTGATGCTGGGCACTGCG-3'); *Esr1* (F 5'- TTATGGGGTCTGGTCCTGCG -3' and R 5'-TCCGTATGCCGCCTTTCATCA -3'); *Esr2* (F 5'- GCCAACCTCCTGATGCTTCT-3' and R 5'- TCGTACACCGGGACCACAT-3'); *Ccna2* (F 5'- CCAAGAGAATGTCAACCCCGAA-3' and R 5'- AGGAAGGTCCTTAAGAGGAGCAA-3'); *AR* (F 5'-GGTCTTCTTCAAAAGAGCCGCTG-3' and R 5'- TTACGAGCTCCCAGAGTCATCCCT-3'); *PGC1α* (F 5'- CCATACACAACCGCAGTTGC-3' and R 5'- ACCCTTGGGGTCATTTGGTGA-3'); *Igf1* (F 5'- CATGCCCAAGACTCAGAAGTCCC-3' and R 5'-AGGTCTTGTTTCCTGCACTTCCTC-3'); Atrogin-1 (F 5'- GACAAAGGGCAGCTGGATTGG-3' and R 5'- TCAGTGCCCTTCCAGGAGAGA-3'); *Murf-1* (F 5'-TGATTCTCGATGGAAACGCTATGG-3' and R 5'- ATTCGCAGCCTGGAAGATGTC-3'); *Col4a1* (F 5'- AAGGGAGAGCAAGGGGTCAG -3' and R 5'-GTACTCCCGGAAATCCAGGTTCA-3'); *Col4a2* (F 5'- TGGGCCCACAACATCAACGA -3'

and R 5'- AAGGCCAGGAAAACCCCGTA -3'); *Col5a1* (F 5'-CAAGCCAGGTTGGCACTGAG-3' and R 5'- CACCTTTCAAACCGCCACTCC-3'); *Lama5* (F 5'- TTCCCACACTGCTACCCTCTG-3' and R 5'- GTCCCAACCTTGGGTCCTTC-3'); *p16* (F 5'- GCTGCGCTCTGGCTTTCGTGAA -3' and R 5'- TGCCCATCATCATCACCTGGTCCAG -3); *p21* (F 5'- CGGTGTCAGAGTCTAGGGGA -3' and R 5'- AGGATTGGACATGGTGCCTG -3), and *Igfbp5* (F 5'- TACCTGCCCAACTGTGACCG-3' and R 5'-ATCCACGTACTCCATGCCCG-3').

RNA sequencing

RNA was extracted from cultured satellite cells using ISOGEN (Nippon Gene) and RNeasy Mini kit according to the manufacturer's instructions. RNA-Seq libraries were prepared using the TruSeq Stranded mRNA Sample Prep Kit setA (Illumina, San Diego CA) according to the manufacturer's instructions, and were subsequently validated for an average size of approximately 330-340 bp using a 2100 Bioanalyzer and the Agilent DNA1000 kit for the construction of sequencing libraries. Sequence data were mapped on the mouse genome (mm10) using Tophat and analyzed by Cufflinks software (http://cole-trapnell-

112 lab.github.io/cufflinks/). The enrichment of gene ontology was calculated by gene ontology

113 tool Database for Annotation, Visualization, and Integrated Discovery (Huang da et al., 2009a,

114 b).

115

116 **References**

117 Fujita, R., Yoshioka, K., Seko, D., Suematsu, T., Mitsuhashi, S., Senoo, N., Miura, S., Nishino,
118 I., and Ono, Y. (2018). Zmynd17 controls muscle mitochondrial quality and whole-body
119 metabolism. FASEB J *32*, 5012-5025.
120 Huang da, W., Sherman, B.T., and Lempicki, R.A. (2009a). Bioinformatics enrichment tools:
121 paths toward the comprehensive functional analysis of large gene lists. Nucleic acids
122 research *37*, 1-13.
123 Huang da, W., Sherman, B.T., and Lempicki, R.A. (2009b). Systematic and integrative
124 analysis of large gene lists using DAVID bioinformatics resources. Nature protocols *4*, 44-57.
125 Ono, Y., Calhabeu, F., Morgan, J.E., Katagiri, T., Amthor, H., and Zammit, P.S. (2011). BMP
126 signalling permits population expansion by preventing premature myogenic differentiation in
127 muscle satellite cells. Cell death and differentiation *18*, 222-234.
128 Ono, Y., Urata, Y., Goto, S., Nakagawa, S., Humbert, P.O., Li, T.S., and Zammit, P.S. (2015).
129 Muscle stem cell fate is controlled by the cell-polarity protein Scrib. Cell Rep *10*, 1135-1148.
130

131